Section A-Research paper

In vitro antibacterial, antifungal, antioxidant, antidiabetic antiinflammatory and anticancer effect of green-synthesized Co_3O_4NPs using *Boerhavia diffusa* plant extract and its physicochemical properties

G.Vanitha[a], R.Manikandan[a,b], A.Prakasam[a,c], M.D.Navinkumar[a,d] , K.Sathiyamoorthi[e], N.Rajendran[f], B.Dhinakaran[a]*

[a]PG and Research Department of Physics ,Government Arts College, Chidambaram ,Tamilnadu, India– 608001.

[b]Munna College of Education, Parangipettai, Tamil nadu, India-608502

[c]PG& Research Department of Physics, Aringar Anna Arts College, Villupuram, Tamilnadu, India-605602

[d]Vivekanadan College of Education, Puducherry, India-605008

[e]PG and Research Department of Chemistry, Government Arts College,Chidambaram , Tamilnadu, India– 608001.

[f]PG and Research Department of Zoology, Government Arts College,Chidambaram , Tamilnadu, India– 608001.

*Corresponding author e-mail: drbdphysics@gmail.com

ABSTRACT

Cobalt is essential to the metabolism of all animals due to its key role in cobalamin, also known as vitamin B12, the primary biological reservoir of cobalt as an ultra-trace element. Current cancer treatment strategies, including chemotherapy and radiotherapy, have been seriously restricted by their side effects and low efficiency for a long time, which urges us to develop new technologies for more effective and much safer anticancer therapies. Novel nanotechnologies, based on different kinds of functional nanomaterials, have been proved to act as effective and promising strategies for anticancer, microbiological, antioxidant, antidiabetic, anti-inflammatory and other treatments. Based on the important biological roles of cobalt, cobalt oxide nanoparticles (NPs) have been widely developed for their attractive biomedical applications. Co_3O_4-Nps were synthesized by using leaf extract of *Boerhavia diffusa* and cobalt nitrate hexahydrate as a source of cobalt. The synthesized NPs were characterized by different techniques such as Ultra-violet spectroscopy (UV), Fourier transform infrared spectroscopy (FTIR), Fluorescence spectroscopy (FL), X-ray diffraction (XRD), Dynamic light scattering (DLS) analysis, scanning electron microscopy (SEM) with EDS and TEM. Electrical property analyzed by cyclic voltammetry (CV). The synthesized Co_3O_4-Nps were evaluated in *vitro* petri plate disc diffusion methods for antibacterial and antifungal activities, anti-oxidant, anti-diabetic, anti-inflammatory studies were done by enzymes denaturation methods, anticancer activity of Co_3O_4-Nps have examined by HepG2 cell line.

Keywords: Green synthesis, *Boerhavia diffusa* , *Co_3O_4NPs*, physicochemical properties, Pharmacological studies

1. INTRODUCTION

Nanotechnology combines various chemical and physical processes to construct nanomaterials, which are less than 100 nm in at least one dimension, and have unique properties

[1]. Nanotechnology has applications across different fields, such as nanomedicines, biomaterials, nanoelectronics, environment, imaging, industries, and agriculture [2,3]. In healthcare, it has been widely used for the diagnosis and treatment of diseases, drug delivery, and novel drug formulations [4]. Cobalt is a transition metal that has a beneficial effect on human health [5,6]. It constitutes a part of vitaminB_{12}, which is useful in anemia treatment as it provokes the formation of red blood cells [6]. Cobalt has unique magnetic, optical, electrical, and catalytic characteristics that make it suitable for a wide range of applications in the field of nanoelectronics and nanosensors [7–9]. Cobalt can exhibit variable oxidation states (Co^{2+}, Co^{3+}, and Co^{4+}), which makes it attractive to be used in several industries [10]. Because of this multivalent state, cobalt has the ability to be present in different spin states in its oxide forms, i.e., low, intermediate, and high [11]. Recently, cobalt nanoparticles (CoNPs) have attracted considerable attention because they are more economical than the noble metal nanoparticle (NP) due to their large surface area [12,13]. CoNPs have been explored as a therapeutic agent for the treatment of diseases, such as microbial infection, which make them attractive for biomedical applications [14,15]. CoNPs are nontoxic in the body at lower levels, have strong activities against bacteria and fungi at lower concentrations, and have fewer side effects than antibiotics [16,17]. Among all NPs, cobalt and cobalt oxide (Co_3O_4) NPs have been exploited the most because of their unique and wide range of applications [18-22]. Co_3O_4 is an antiferromagnetic p-type semiconductor with a direct optical band gap of 1.48 and 2.19 eV [23, 24]. Co_3O_4 is a multifunctional material and has many biomedical such as applications (antibacterial, antiviral, antifungal, antileishmanial, therapeutic agents, anticancer, and drug delivery), gas sensors, solar selective absorbers, anode materials in lithium-ion batteries, energy storage, pigments and dyes, field emission materials, capacitors, heterogeneous catalysis, magneto-resistive devices, and electronic thin films [25–29]. The oxides of cobalt are abundant in nature, as only the Co_3O_4 and CoO are stable [30], with Co_3O_4 possessing the highest stability. *Boerhavia diffusa* is a widely distributed plant occurring throughout India, the Pacific, and southern United States. *Boerhavia diffusa* is commonly known by the name *Punarnava* in India, *Mookirattai* in Tamil Nadu, Punarnavine, an alkaloid isolated from this plant has been shown in vitro to possess anti-cancer, anti estrogenic, anti amoebic and immune modulatory activities [31]. The leaves of *Boerhavia diffusa* are often used as a green vegetable in many parts of India and are very well known to possess medicinal properties. They are generally used for pain relief and to protect and improve eyesight. Extracts of *Boerhavia diffusa* leaves have been shown to possess antioxidant, hepato protective, diuretic and anti-diabetic properties in pharmacological models [32]. In this study, we report for the first time *Boerhavia diffusa* extract as an effective chelating agent for the facile and rapid bio-synthesis of pure Co_3O_4 single-phase nanoparticles at a low temperature. The fact that there was no use of inorganic/organic solvents neither surfactants nor high temperature makes this synthesis an effective green and eco-friendly process. The bioinspired Co_3O_4NPs characterization was broadly done by UV, FTIR, FL, XRD, SEM, EDS, TEM, and CV. Moreover, the antibacterial, antifungal properties, antioxidant, antidiabetic, anti-inflammatory and anticancer potency of Co_3O_4NPs have been studied *in vitro* methods.

2. Materials and methods

2.1. Collection of Sample

Fresh and healthy leaves of *Boerhavia diffusa* (Mookirattai) were collected from botanical garden, Government Arts College, Chidambaram. Leaves were washed in three times thoroughly by running ordinary tap water (OTW), then washed two times with double distilled water (DDW) to remove any dust particles on the leaves. Washed leaves were allowed to dry in

air at room temperature. The dried leaves were grained and powdered by using electric mixer. This powder was used to prepare the leaves extracts

2.2. Chemicals, Solvents and Starting Materials

De-ionized water, whatmann 1≠ and whatmann 41≠ filter papers, cobalt nitrate hexa hydrate ($Co(NO_3)_2$. $6H_2O$, Sodium hydroxide pellets, hydrochloric acids, sulphuric acid, vitamin C, Acrobose, Diclofenac sodium, Muller Hinton agar(MHA), Sabouraud Dextrose agar(SDA), sodium phosphate, ammonium molybdate, Amylase, DNSA reagent, Dimethyl formamide, Bovine serum albumin solution, 3-[4, 5-dimethylthiazol-2-yl]-2, 5-diphenyl tetrazolium bromide, tetrazolium, phenol red, DMSO, and other chemicals were purchased from Merck (India) Ltd. All chemicals were used without further purification.

2.3 Instruments and equipment

Electric oven, Magnetic stirrer (REMI 2 MLH), E-1 portable TDS & EC meter,pH-009(I)A pen type pH meter, petri plate, ordinary incubator, CO_2 incubator, Micro Plate reader, Inverted microscope, Refrigerated centrifuge, sterilized 250ml separating funnels, sterilized conical flasks, sterilized 400ml beakers, watch glasses, 7'' funnels, glass rods, and 10ml measuring cylinders,

2.4. Plant material processing

5 grams of healthy *B. diffusa* healthy leaves powder with 50 mL of double-distilled water (DDW) taken in the 250 mL round bottomed flask, water condenser fitted and fix the running tap water then heated for 20 min at 80^O C. Then the extract was filtered with Whatman 1≠ filter paper. The filtrate was used for further green synthesis of process

2.5. Biosynthesis procedure

For the synthesis of Cobalt oxide nanoparticles by reducing cobalt nitrate hexahydrate (M.F:$Co(NO_3)_2.6H_2O$, MW: 291.04 g/mol), 180 mL of homogenous solution of cobalt nitrate is steadily mixed with 10mL of leaves extract followed by continuous heating (70 °C) and stirring at 500 rpm for 3 hr at magnetic stirrer with heating instrument, to achieve reddish pink solution [33-35], The obtained brownish red colour solution was added with 0.1M NaOH solution maintain by pH 10, the solution was changed to blue colour precipitate. The obtained precipitate was filtered by whatmann 1# filter paper. The precipitate was dried and powdered then calcinated at 350^oC through muffle furnace. After calcination to obtained gray colour fine crystalline cobalt oxide nanoparticles. Finally, Co_3O_4NPs were steadily characterized. Figure.1, have shown in scheme of green synthesis of cobalt oxide nanoparticles.

2.6. Characterization of Co_3O_4 nanoparticles

2.6.1. UV–Vis spectroscopy

To observe the absorption maximum of biosynthesized Co_3O_4NPs, samples were analyzed for UV–vis spectroscopic studies (Perkin Elmer UV/vis, Lambda 35 spectrophotometer) at room temperature operated at a resolution of 1 nm between 190 and 1100 nm ranges.

2.6.2. FT-IR spectroscopy

Co_3O_4NPs were investigated by Fourier transform IR spectroscopy with a PerkinElmer Spectrum Two, Fourier transform IR system with a frequency ranging from 400 to 4000 cm^{-1} and a resolution of 4 cm^{-1}. The KBr pellet method was used to prepare the samples

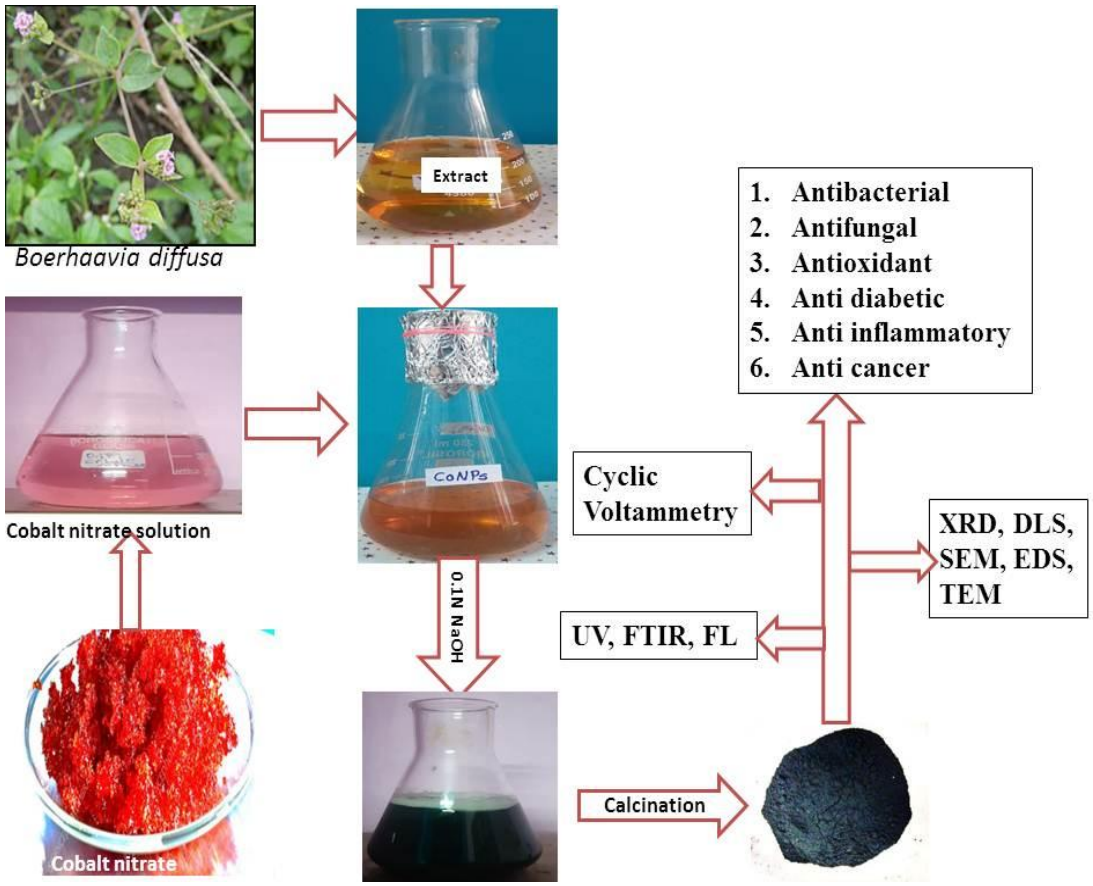

Figure:1 Scheme Green synthesis of cobalt oxide nanoparticles by *Boerhavia diffusa*, spectral characterization, Morphological, electrical and Pharmacological studies

2.6.3 Fluorescence spectroscopy

The fluorescence intensity was recorded while the emission wavelength was scanned from 200 nm to 900 nm with fixed excitation of 420 nm using a Perkin Elmer spectro fluorometer, LS 45.

2.6.4. X-ray diffraction study

The solid state dispersions of Co_3O_4NPs were evaluated with X-ray powder diffraction. Diffraction patterns were obtained using an XPERT-PRO diffractometer (PAN analytical Ltd., the Netherlands) with a radius of 240 mm. The Cu Ka radiation (Ka 1.54060 A°) was Ni filtered. A system of diverging and receiving slits of $1^o$and 0.1 mm, respectively, was used. The pattern was collected with 40 kV of tube voltage and 30 mA of tube current and scanned over the 2h range of $10–90^o$.

2.6.5. Dynamic light scattering (DLS)

DLS analysis was done with a Micromeritics (Nano Plus) according to standard method with some modifications. The instrument can measure (Dilution Method) the particle size of samples suspended in liquids in the range of 0.1 nm to 12.3 μm with sample suspension concentrations from 0.00001% to 40%, and a sensitivity for molecular weight to as low as 250 Da. The concentration of the Co_3O_4NPs was 100 lg/mL sonicated for 2 min, and dynamic particle sizes were measured by suspending two drops of an aqueous suspension of NPs in 10 mL of Millipore water. When the NPs had completely dispersed in water, they were analyzed with a DLS analyzer. The experiments were repeated several times to obtain the average size of the NPs.

2.6.6. Scanning electron microscopy

The particle size and microstructure were studied by high resolution scanning electron microscopy (SEM; instrument from Nikon, Japan). In brief, Ag NPs were suspended in deionized water at a concentration of 1 µg/ml and then sonicated using a sonicator bath until the sample forms a homogenous suspension. For size measurement, the sonicated stock solution of Co_3O_4NPs (1 µg/ml) was diluted 20 times. Then one drop of sonicated aqueous solution was taken on a glass plate and dried it. Then the sample was gold coated and images were taken. SEM was used to characterize the size and shape of Co_3O_4NPs.

2.6.7 EDS

This technique determines the elemental composition of a sample. In this study it was used to confirm the presence of cobalt in the particles as well as to detect the other elemental compositions of the particles. Beside identification of the elements present in the sample by the use of EDS it is also possible to estimate their concentration. The particle solution was diluted 100-fold in water and a drop of 10 lL diluted solution was placed on a carbon stub and air-dried. The EDS spectrum was obtained at an acceleration voltage of 20 kV and collected for 19 s. Mapping was completed using pseudo-colors to represent the two-dimensional spatial distribution of energy emissions of the chemical elements present in the sample. Analysis was done using JEOL JSM 6360 equipped with an EDS analyzer.

2.6.8. Transmission electron microscopy

The particle size and microstructure were studied by high resolution transmission electron microscopy in a JEOL 3010, Japan, operating at 200 kV according to the method of with some modifications. In brief, Co_3O_4NPs were suspended in deionized water at a concentration of 1 µg/ml then the sample was sonicated using a sonicator bath until sample forms a homogenous suspension. For size measurement, sonicated stock solution of all Co_3O_4NPs (0.5 µg/ml) was diluted 20 times. TEM was used to characterize the size and shape of the Co_3O_4NPs. A drop of the aqueous Co_3O_4NPs suspension was placed on to carbon-coated copper grid and this was dried in the air to get TEM image.

2.7 Cyclic voltammetry studies

Cyclic voltammetry analysis done by Versa STAT MC (Princeton Applied Research), Frequency range: 1Hz to 1MHz, Electrochemical characterization of the green synthesized cobalt oxide nanoparticles carried out by using cyclic voltammetry (CV). Cyclic voltammetry measurements were carried out by using drop sense software driven mini PGSTAT302. The screen print electrode consists of three electrodes which are Ag/AgCl as reference electrode, counter electrode and a carbon working electrode. The carbon electrode (working electrode) was modified using the drop-dry method. Separate drop of Co_3O_4NPs was cast on the electrode respectively and dried in the oven for 2 min at temperature of 50°C. The voltammogram for the bare and modified SPC electrode were measured in 5mM potassium hexacyano-ferrate (III) ($K_3Fe(CN)_6$) solution prepared in 0.1Mphosphate buffer solution (PBS) as a supporting electrolyte.

2.8. Antibacterial assay

Four pathogenic bacterial strains, two gram positive (*Staphylococcus aureus*, *Escherichia coli*,) and two gram negative (*Pseudomonas aeruginosa*, *Bacillus cereus*) were used in this assay. The bacterial strains were collected from microbiological department of Center of Advanced Study (CAS) in Marine Biology, Annamalai University, Portonova. Bactericidal activity was determined by using disc diffusion method. Bacterial cultures were refreshed in nutrient broth for 24 h at 37^{o}C. Nutrient agar medium was used for the growth of bacterial strains. Filter paper discs of 6 mm in size ware prepared from whatman no. 1 filter paper. Media, filter paper discs

along with other apparatus required in this assay were autoclaved for sterilization and experiment was performed in microbiological safety cabinet. Bacterial strains were streaked on solidified labeled nutrient agar plates. Ampicillin was used as standard drug. Then 20 mg of samples were loaded per disc, placed on respective places in petri plate and incubated for 24 h at 37^{o}C for antibacterial activity. Zones of inhibitions were measured after 24 h.

2.9. Antifungal assay

Fungicidal activities of synthesized Co3O4NPs by *B.diffusa* were measured by observing the growth response of two fungal strains (*Candida albicans*, *Trichoderma viride*). The fungal strains were collected from Center of Advanced Study(CAS) in Marine Biology, Annamalai University, Portonova. Sabouraud dextrose broth was used for refreshing fungal culture and grown on sabouraud dextrose agar (SDA). Modified method was followed for measuring the fungicidal capacities. All apparatus were autoclaved for sterilization. Experiment was performed in triplicate and carried out in microbiological safety cabinet. Sample solution was absorbed on discs and placed on respective labeled solidified SDA plates. Amphotericin B was used as standard drug and 20 mg per disc of nanoparticles was used for antifungal activity. Plates were incubated for 24 h at 28^{o} C and zone of inhibition around the discs were measured.

2.10 Anti-oxidant studies by DPPH method

Antioxidant potential of Co_3O_4NPs against DPPH was determined using the method with slight modification. DPPH assay was performed in 96 wells plate. Test sample (20 ml) from stock solution was poured in respective well of plate and then 180 ml of DPPH solution was added in each well to make 200 ml final volume. Ascorbic acid was used as reference standard. Mixture was incubated at room temperature for half an hour. Change in color from violet to yellow was observed due to the antioxidation potential. Absorbance of reaction mixture was measured at 517 nm on microplate reader. Scavenging activity was calculated by given equation.

$$\% \text{ Scavenging} = \frac{OD\ of\ control - OD\ of\ test\ sample}{\text{OD of control}} X\ 100$$

OD=optical density absorbance

2.11 Anti-diabetic activity

α-amylase inhibition technique

The antidiabetic activity of the samples was performed using α-amylase inhibition method. Briefly, Amylase (0.2%) was incubated with and without samples (in 1.5 mL) and standardized for 10 min at 25◦C. This experiment was performed in 0.2M phosphate buffer (pH 6.9). After pre incubation, the 1% starch solution (0.5mL) was added and the reaction mixture was incubated for 30 min at 25◦C. In order to stop the enzymatic reaction, DNSA reagent (0.5 mL) was added as the color reagent and then incubated in a boiling water bath for 90 min. After cooling down to the room temperature, 0.5 mL of samples was diluted to 2.5mL of distilled water and the absorbance measured at 540 nm using a UV-Visible spectrophotometer. The measured absorbance was compared with that of the control experiment. The percentage inhibition was calculated from the given formula.

% of Inhibition = 100 x[Ac-At /Ac]

At: Absorbance of test

Ac: Absorbance of control

2.12 *In vitro* anti-inflammatory activity

BSA denaturation technique

The synthesized compound and standard diclofenac sodium were screened for anti-inflammatory activity by using the inhibition of albumin denaturation technique with minor modification. The standard drug and compound were dissolved in minimum quantity of

Dimethyl formamide (DMF) and diluted with phosphate buffer (0.2 M, PH 7.4). The final concentration of DMF in all solution was less than 2.5%. Test Solution (2.5 mL) containing different concentrations of the drug was mixed with 1 mL of 1 mM Bovine serum albumin solution in phosphate buffer and incubated at 37 °C in an incubator for 10 min. Denaturation was induced by keeping the reaction mixture at 70°C in a water bath for 10 min. After cooling, the turbidity was measured at 660 nm. Percentage of Inhibition of denaturation was calculated from control where no drug was added. The percentage inhibition of denaturation was calculated by using the following formula.

$$\% \text{ of Inhibition} = 100 \times [Ac-At/Ac]$$

At: Absorbance of test

Ac: Absorbance of control

2.13 Anticancer activity

Cell viability assay/MTT Assay

The human hepatic carcinoma cell line (HepG2) was obtained from National Centre for Cell Science (NCCS), Pune, India and grown in Eagles Minimum Essential Medium containing 10% fetal bovine serum (FBS). The cells were maintained at 5% CO_2 and incubated at 37 °C for 24 hours. After 24 h the cells were treated with serial concentrations of the test sample (cobalt oxide nanoparticles) (6.25, 12.5, 25, 50, and 100 µg/ml) and placed in the humidified 5% CO_2 incubator for 48 h. Cells incubated in culture medium alone served as a control for cell viability (untreated wells). Each experiment was repeated at least three times. After cobalt oxide nanoparticles treatment, cells were aspirated by 600 µL of phosphate buffer saline (PBS) (pH 7.0) and centrifuged for 10 min at 3000 rpm to remove cell debris and obtain a clear supernatant.

$$\% \text{ Cell viability} = [A] \text{ Test} / [A] \text{ control} \times 100$$

3. Result and discussion

3.1 UV Spectral analysis

UV-Vis spectroscopy result showed that the typical peaks of Co3O4 NPs were detected in the range of maximum wavelength between 200-350 nm and 380-600 nm as shown in Fig. 1b. These peaks indicated the transfer processes of Co (II) and Co (III) with oxygen, respectively [36]. Figure 2a shows the absorption spectrum of the synthesized Co_3O_4NPs with the absorption peak around 395.05 nm [37]. It indicates that Co_3O_4NPs displays excitation absorption (at 261 nm) due to their large excitation binding energy at room temperature. The sharp bands of cobalt colloids were observed at 261 nm, which proves that the cobalt ion is efficiently reduced by the *Boerhavia diffusa* leaf extract.

3.2. FTIR Analysis

FTIR analysis for the biogenically synthesized, Co_3O_4NPs and the leaf extract of *Boerhavia diffusa* were carried out in order to explore the formation of Co_3O_4NPs and confirm the functional groups present in the aqueous leaf extract. This in turn enables to identify the bioactive molecules which were actively involved during the synthesis process as stabilizing and capping agents [38-40] to prevent the overall growth of Co_3O_4NPs. **Figure 2(b-c)** shows the FTIR spectra of aqueous leaf extract of *Boerhavia diffusa* and Co_3O_4NPs by *Boerhavia diffusa* and were recorded in the range of 4000–400 cm^{-1}. The FTIR spectrum of aqueous leaf extract of *Boerhavia diffusa* have shown in(Figure:2b), the broad peak observed in the spectrum at around 3436 cm^{-1} O-H stretching with a C=O peak, 2923 cm^{-1} represents the C-H stretching vibration, the strong peak of 1645 cm^{-1} reveals that carbonyl group, the vibration of 1385 cm^{-1} have shown in C=C stretching vibration, the vibration of 1035 cm^{-1} have indicates overlapping of aliphatic

amines, =C-H & $=CH_2$ (out-of-plane bending). The bending vibration of 787 and 602 cm^{-1} have shown in ring strain for carbon chain.

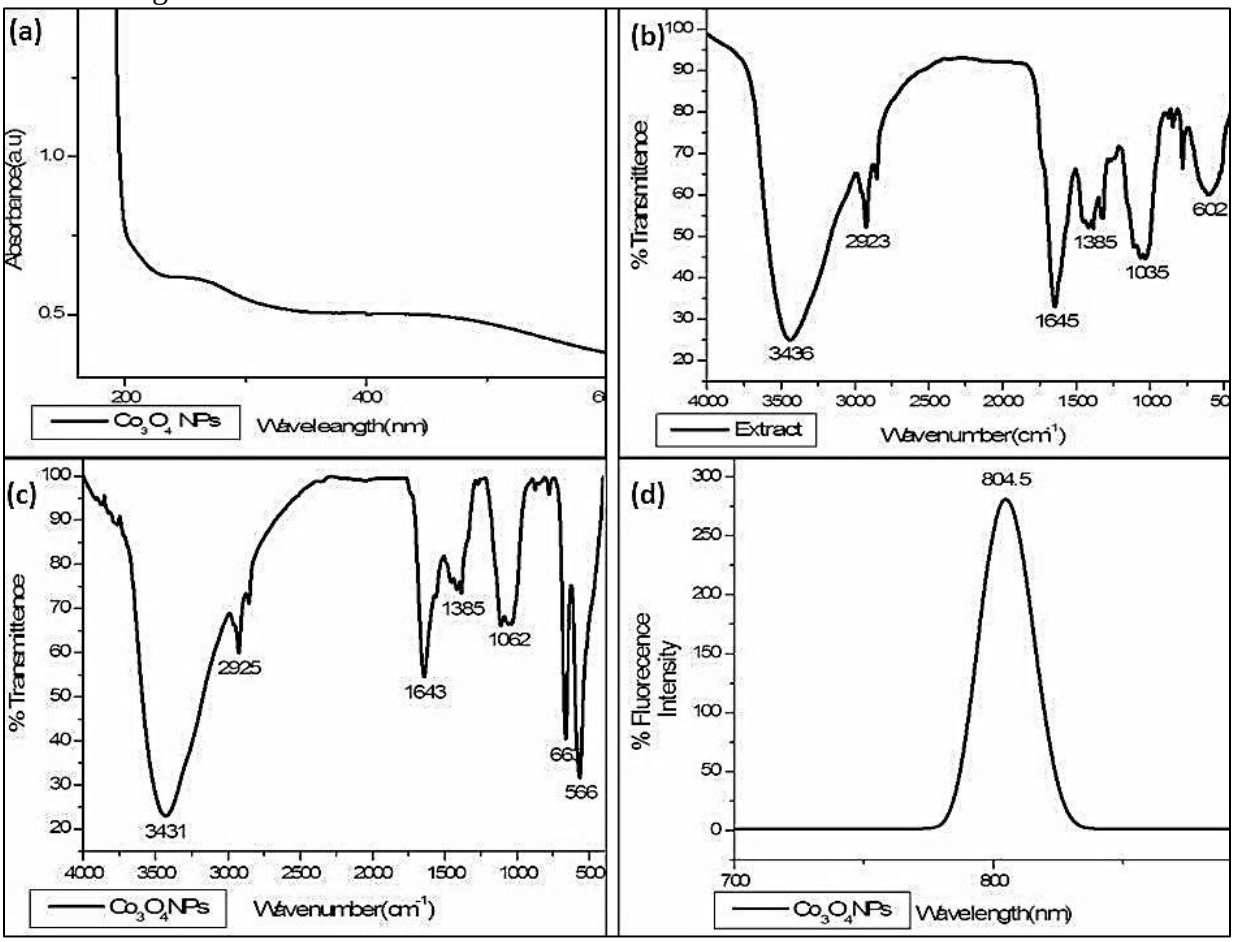

Figure:2. (a)UV spectrum of Co_3O_4NPs, (b) FTIR spectrum of *Boerhavia diffusa leave extracts,* (c) FTIR spectrum of Co_3O_4NPs by *Boerhavia diffusa* leaves extract, (d) Fluorescence spectrum of Co_3O_4NPs by *Boerhavia diffusa* leaves extract

The FTIR spectrum of *Boerhavia diffusa* leaves extracts capped Co_3O_4NPs, showed absorptions at The IR spectrum of cobalt oxide exhibits two major bands at 662 cm^{-1} and 566 cm^{-1}, this doublet sharp peak reveals that spinal structure of Co_3O_4NPs. The first band is associated with the Co^{3+} vibration in the octahedral hole and the second band (ν) is attributed to the Co^{2+} vibration in the tetrahedral hole, which confirms the formation of the Co_3O_4 spinel. The frequency of 1062 cm^{-1} have shown in -C-C-C- bending vibration, 1385 cm^{-1} have evident that deformation of $-CH_2-$ and $-CH_3$ bending vibrations, 1643 cm^{-1} have indicates carbonyl stretching vibration, the weak peaks at 2925 cm^{-1} indicates some of the groups like alkyl, alcohols and amide are reduced and merged. The sharp and broad band of 3431 cm^{-1} have indicates –OH group, this band very sharpen compared to leaves extract because many carbonyl functional groups are reduced to form alcohol and increases the number of –OH groups. The excess peaks of 3780 and 3865 cm^{-1} indicates to the free –O-H groups. It's come from, during the nanoparticles synthesis, sodium hydroxide was added due to maintain the pH ~10. The above three FTIR spectrum were reveals that leave powder spectrum having more phyto-constituents, Aqueous extract spectrum have shown only the water soluble phyto constituents, finally cobalt nanoparticles FTIR shown the reduced peaks cobalt ions(Co^{3+} and Co^{2+}) ions reduced the various

phyto-constituents. It is possible to elucidate the formation of Co_3O_4 NPs with many surface hydroxyl function groups

3.3 Fluorescence Spectra analysis

In this study, we have investigated the fluorescence emission spectra of Co_3O_4NPs. The spectral characteristics of fluorophores must match the wavelengths of the excitation light, Dichroic and emission filters of the fluorescence microscope on which the experiments are to be done. Moreover, it is advised that their spectra are well separated from the spectra of other fluorophores that will be used simultaneously in the experiments to minimize cross-talk and bleed through, which can give rise to [41] false co-localization and misinterpretations if not appropriately corrected. For use with advanced optical techniques (such as higher solution microscopies, two-photon microscopy, fluorescence lifetime imaging, spectral imaging or correlation spectroscopy), further photo-physical aspects (e.g., lifetime, blinking, and environmental sensitivity) must also be taken into account. Figure:2d shows the fluorescence emission of cobalt nanoparticles by aqueous leaves extracts of *Boerhavia diffusa* , It shows that the plasmonic resonance in the range close to 804.5 nm

3.4 XRD Analysis

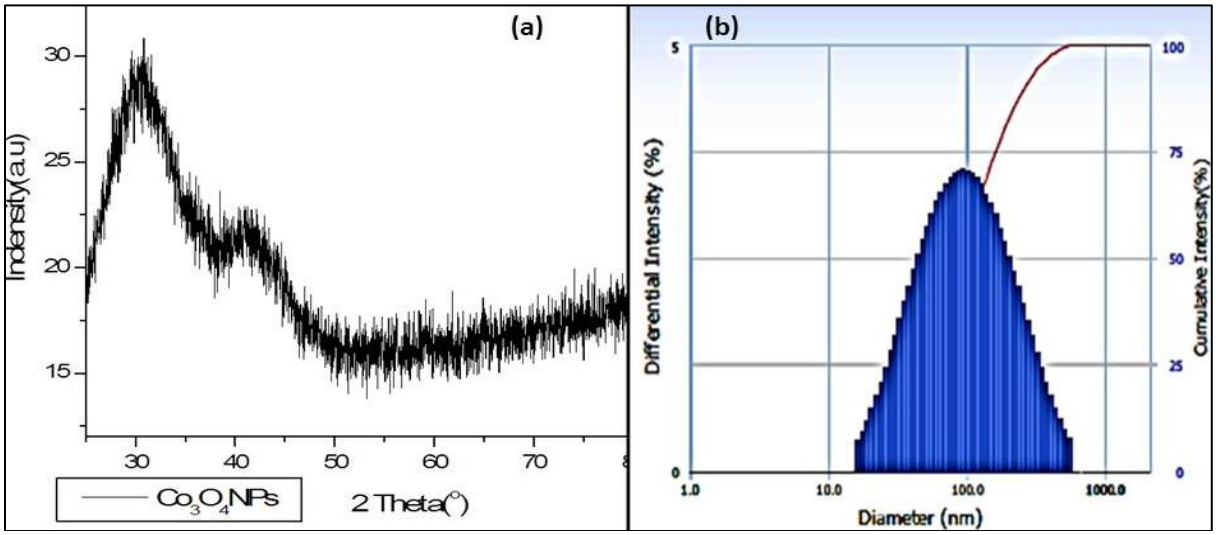

Figure 3. (a) XRD Pattern of Co_3O_4NPs by *Boerhavia diffusa* leaves extract, (b) DLS results image of Co_3O_4NPs by *Boerhavia diffusa* leaves extract

X-ray diffraction (XRD) technique was used to determine the purity and phase of the powdered Co_3O_4NPs from aqueous leaves extract of *Boerhavia diffusa*. Fig. 3a represented the typical diffraction pattern in which the peaks at 2θ were 31.28, 36.76, 59.28 A0 corresponds to Co_3O_4 having spinel structure and cubic close packed phase [JCPDS card no.–01-073-1701]. Insignificant peaks observed could be attributed to organic substances. A shift in some peaks was due to the presence of impurities owing to the biomass residue [42]. The presence of broad peaks suggests the synthesized particles to be very small in size in the nano dimensional state and amorphous in nature. The average crystallite size determined by the Scherrer formula, $D = 0.9\lambda/\beta \cos\theta$ using the half-width of the intense peak in the powder pattern. Where D is the crystallite size, λ is X-Ray wavelength which is 1.54 A0, β is full width at half maxima (FWHM) and θ is Bragg's angle.

The crystallite size of biologically synthesized Co_3O_4 NPs corresponding to the highest peak observed in XRD pattern was approximately 55.8 nm. The average crystallite size was found to be in the range of (1.5-96 nm). This belongs to Co element present and it makes the

nanoparticles smaller (4.9nm). Depending on the XRD analysis, Aliyaa A. Urabe et al refer to synthesis of cobalt nanoparticles with 21-74 nm by *Camellia sinensis* extracts[43]. Malathy et al, refer to synthesis of cobalt nanoparticles with 50 nm by *Cadiospermum halicacebium* leaves extract [44]. This difference in size belongs to differ in reducing agents (plant extracts). Number of Bragg values are Co_3O_4NPs by *Nyctanthes arbor-tristis* (Pavalamalli) leaves (111, 220, 311, 222, 400, 422, 511, 531) XRD pattern indicates that the cobalt oxide nanoparticles

3.5 DLS analysis

DLS is the most often applied technique to determine the distribution of Co_3O_4NPs size in its condensed state[45]. The evaluated result of Co_3O_4NPs particle size shows the size variation range mendacities amongst 20 and 700 nm with highest size variation around 99.8 nm as shown in Figure 3b. Comparatively the size variation diagrams in DLS analysis have good symmetry and reveals the homogeneity of resultant Co_3O_4NPs. Particles of the Co_3O_4NPs have reveals that during the measurement of DLS analysis, the nanoparticles of cobalt oxide were associated to aggregate. This is reasons for particle sizes are increased.

3.6 SEM analysis

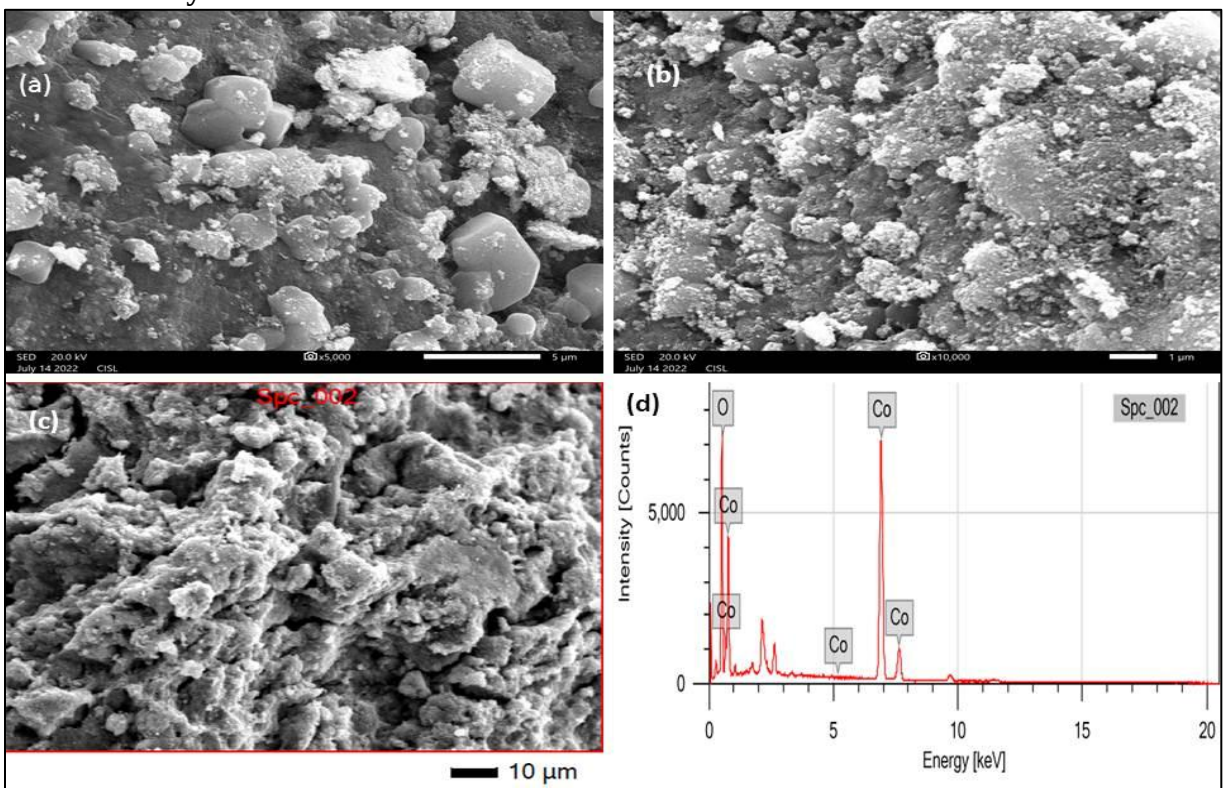

Figure 4. (a-b) SEM Images of Co_3O_4NPs by *Boerhavia diffusa* leaves extract, (c) EDS micrograph image of Co_3O_4NPs, (d) EDS image of Co_3O_4NPs by *Boerhavia diffusa* leaves extract

SEM micrographs with high magnification were used to determine the morphology and grain size of all calcined Co_3O_4 NPs. The highly magnified micrograph (figure 4 (a-b)) clearly shows that the small particles joined together forming a bunch like structure, where clear boundaries among the particles were seen [46]. Spherical like particles, mountain rock shaped poly crystalline particles also seen. The particle sizes estimated from SEM micrographs using Image J software are 5µm in figure 4a, 1µm in figure 4b.

3.7 EDS analysis

To check the chemical composition of synthesized Co_3O_4NPs was measured by EDS analysis. Figure.4a have shown similar results like SEM analysis, both the image have shown in cluster like structure[46], The spectrum shows the strong EDS peaks associated with Co and O elements in CoO in nanoparticles and other peaks are also obtained in EDS which may be due to the chemicals which were added during processing of nanoparticles were found in the EDS spectrum as shown in Fig.4b. This result shows the percentage of all elements present in the nano particles

3.8 Transmission electron microscopy

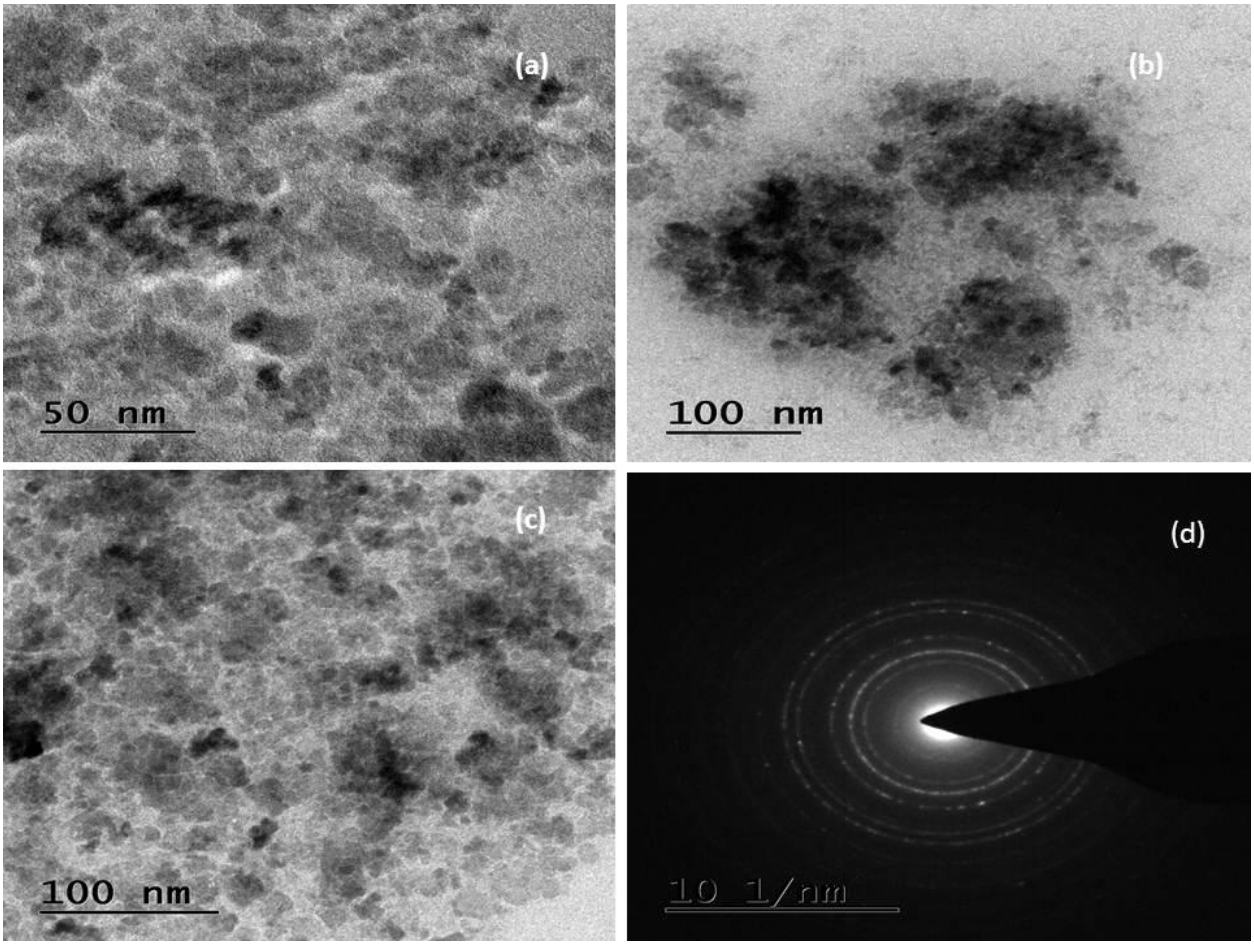

Figure:5(a-c) TEM Image of Co_3O_4NPs by *Boerhavia diffusa* leaves extract, (d) SAED Pattern of Co_3O_4NPs by *Boerhavia diffusa* leaves extract

TEM images of the obtained samples (Figure 5) reveal a polycrystalline nature. The TEM images show that there is not a well-defined and uniform shape. However, a tendency toward polycrystalline shapes is observed. A closer look at the crystal edges also reveals trigonal, pentagonal and hexagonal shapes. The crystallite sizes revealed by TEM are in the figure 5a and 5b have shown in 1µm sized cobalt oxide nanoparticles, figure 5c have shown in 100 nm. This roughly corroborates the estimates from XRD, DLS and SEM analysis which, for instance, provided values of 100 nm for above three analyses. In the literature, Co_3O_4 particles have been synthesized with various morphologies such as hollow nanospheres [47], nanowires [48],

nanotubes [49,50] and octahedrons [51]. The properties of Co_3O_4 nanoparticles are known to vary with their shape, size and crystallization conditions.

3.9 Electrochemical studies

The electrochemical behaviour of Co_3O_4NPs by *Boerhavia diffusa* leaves extract was tested with cyclic voltammetric (CV) measurements in 0.1 M KOH. Figure 6a shows the CV of Co_3O_4 mediated by *Boerhavia diffusa* in KOH electrolyte. It can be seen that the Co_3O_4 is non-electro active in the selected potential region. The broad peaks in the potential range from −1 to -0.5 V. It shows the cathodic peak at -1.5 V with enhanced current response relative to that of Co_3O_4 by *Boerhavia diffusa*. At the same time, we have noticed that the Co_3O_4 by *Boerhavia diffusa* shows higher current response at the positive potential region 0 to 1.5 V, which was indicative of the electron transport property of nitrobenzene.

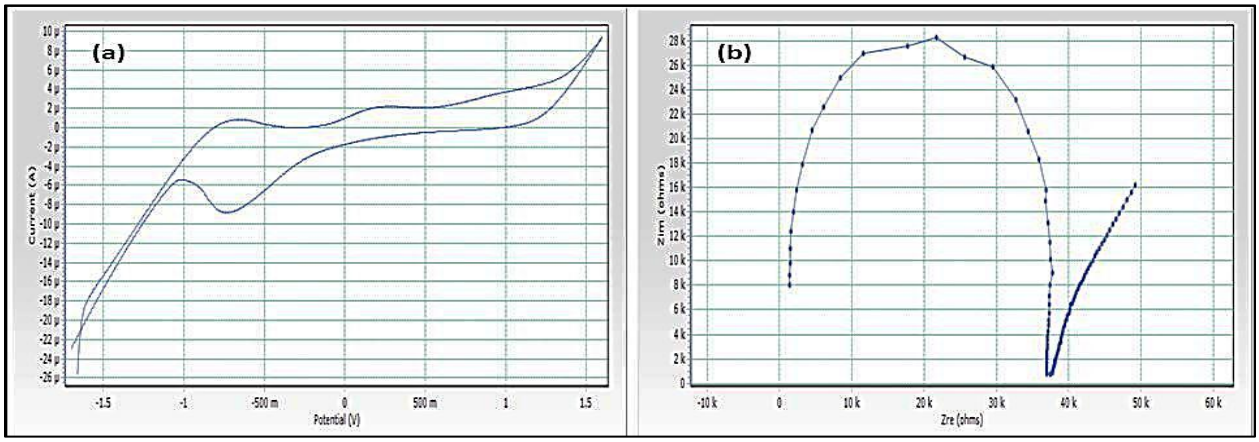

Figure:6 (a) Cyclic Voltammograms of Co_3O_4NPs by *Boerhavia diffusa* leaves extract, (b) Electrochemical Impedance Spectrum (EIS) of Co_3O_4 nanoparticles by *Boerhavia diffusa* leaves extract

Figure 6(b) demonstrates the Co_3O_4 electrode Electrochemical Impedance Spectroscopy. The ionic motion between the electrode and electrolyte surface was observed by EIS within the frequency range 1Hz to 100 kHz through 5 mV of amplitude [52-53]. Apparently, the Co_3O_4 electrode charging transfer resistance is very small, which indicates that effective electrochemical reaction sites are enough. Additionally, the Co_3O_4 electrode's diffusion resistance is lower, enabling the diffusion of ions in the redox reaction phase.

3.10 Antibacterial activity

Antibacterial activities of synthesized Co_3O_4 NPS have shown in Figure:7(petri plates), Figure 8 have shown in cluster column chart of antibacterial activity of Co_3O_4 NPs by *Boerhavia diffusa* . The antibacterial activities were studied amongst both (Gram positive and Gram negative) pathogenic bacteria. Co_3O_4NPs showed maximum zone of inhibition against *Staphylococcus aureus* (12 mm) at 1000 µg/ml concentration this is excellent antibacterial activity of Co_3O_4 NPS mediated by *Boerhavia diffusa* , Co_3O_4 NPs have shown good antibacterial activity against *Escherichia coli* (10 mm at 1000 µg/ml) and against *Bacillus cereus* bacterial strain. The results also have shown that even if the concentration increases, the activity of zone of inhibition does not change in three different concentrations (1000µg/ml, 750 µg/ml and 500 µg/ml) of the test solutions[54]. Antibacterial activity of Co_3O_4 NPs have shown unchanged (8 mm) for Pseudomonas strains in three different concentrations of test solutions (1000µg/ml, 750 µg/ml and 500 µg/ml), this is shown in moderate activity compared with standard antibacterial drug. The zone of inhibition values have shown in Table:1.

Table:1 Antibacterial and antifungal activity of Co_3O_4NPs by *Boerhavia diffusa*

Organisms		Zone of Inhibition (mm)			
		Sample (µg/ml)			Standard
		1000	750	500	
Bacterial strains	*Staphylococcus aureus*	12	10	8	8
	Escherichia coli	10	7	7	12
	Pseudomonas	8	8	8	13
	Bacillus cereus	13	13	13	16
Fungal strains	*Candida albicans*	14	8	8	12
	Trichoderma viride	9	9	9	17

3.11 Antifungal activity

The antifungal activity of Co_3O_4 NPs by *Boerhavia diffusa* have shown excellent activity(12 mm) at 1000 µg/ml, moderate activity(8mm) at 750 µg/ml and 500µg/ml, against *Candida albicans* fungal strain[54]. Moderate and same antifungal activity has been shown in *Trichoderma viride* fungal stain(9mm) at three concentrated test solutions(1000 µg/ml, 750 µg/ml and 500 µg/ml) of Co_3O_4 NPs containing test solutions. Anti-fungal activity have shown in figure 7, Cluster column chart of antifungal activity have shown in figure 8, and the zone of inhibition values have shown in Table.1.

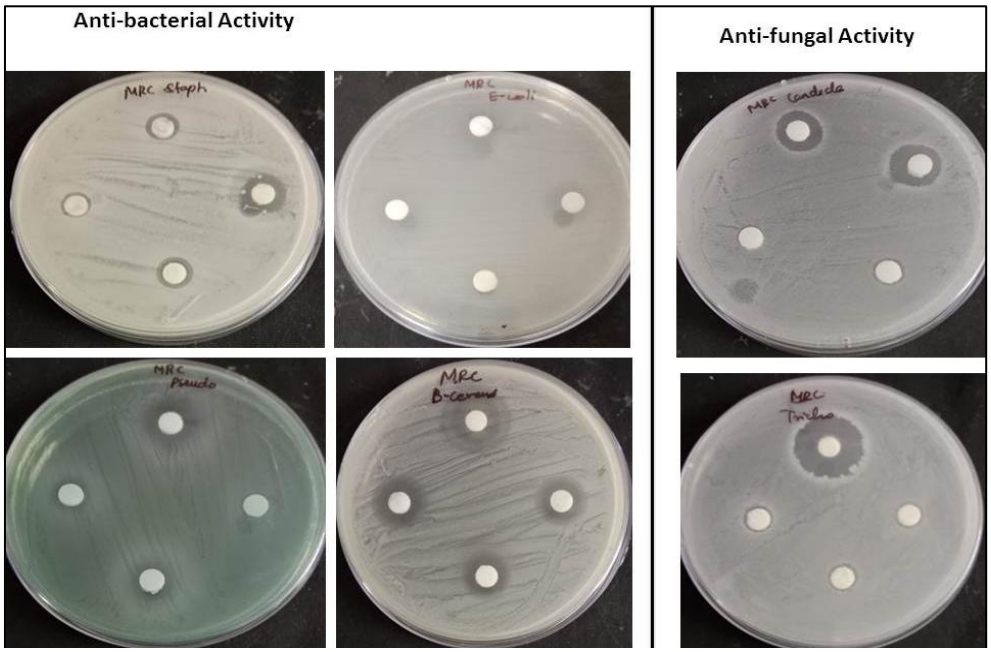

Figure:7 Anti-bacterial and antifungal activity of Co_3O_4NPs by *Boerhavia diffusa* leaves extract

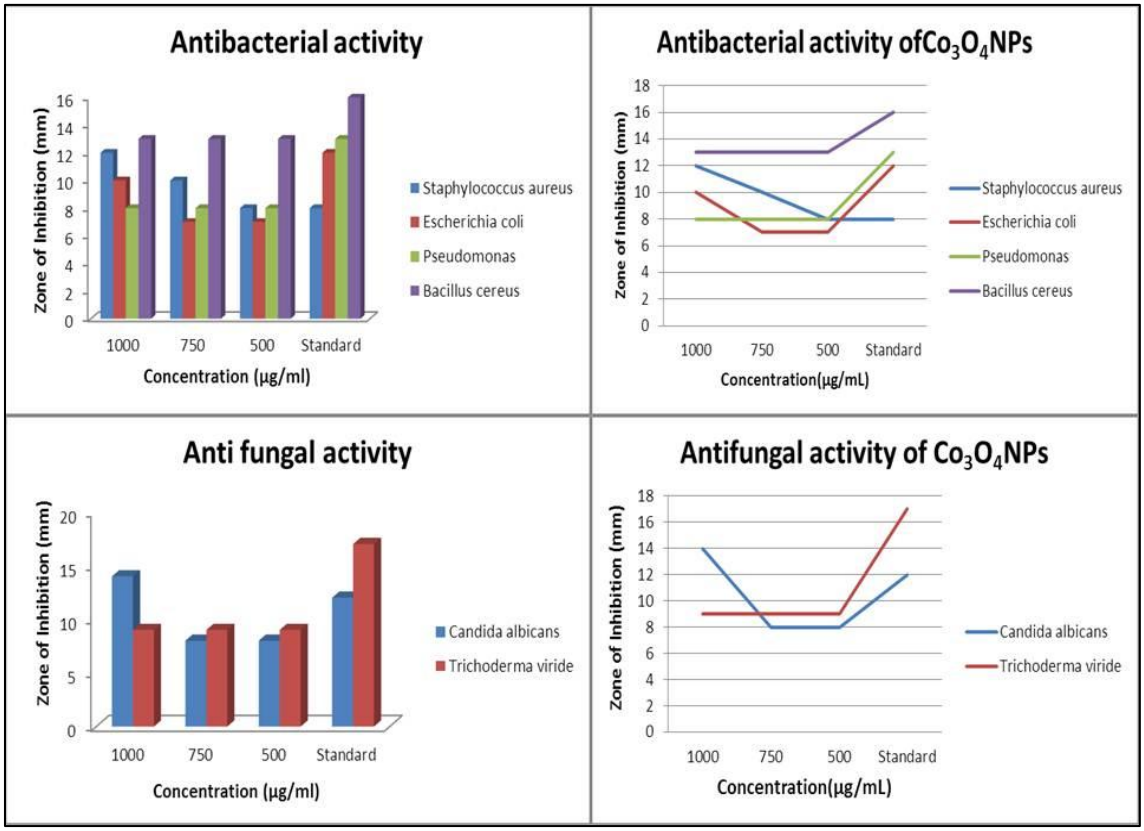

Figure:8 The cluster column chart of antibacterial and antifungal activity of Co_3O_4NPs by *Boerhavia diffusa* leaves extract

3.12 Antioxidant activity

The results confirmed the Co_3O_4 NPs and vitamin C has the antioxidant activity. The Co_3O_4 NPs has 29.55% antioxidant activity[55] while vitamin C has 24.28% antioxidant activity. The results confirmed the Co_3O_4 NPs has greater antioxidant activity as compared with vitamin C (Fig. 9).

Table:2. Percentage of inhibitory concentration of Antioxidant, Antidiabetic and anti-inflammatory activity of Co_3O_4NPs by *Boerhavia diffusa* leaves extract

Concentration (µg/mL)	% of inhibitory concentration					
	Antioxidant activity		Antidiabetic activity		Anti inflammatory activity	
	Co_3O_4NPs	Vitamin C	Co_3O_4NPs	Acarbose	Co_3O_4NPs	Diclofenac sodium
50	5.4050	31.3725	22.2564	29.1282	28.5536	22.3192
100	10.2564	50.7042	35.2821	45.4359	39.7756	35.6608
200	18.6047	83.1731	50.5641	60.2051	49.6259	45.5112
250	25.5319	92.5373	72.0000	77.7436	63.4663	57.3566
500	32.6923	96.7290	75.4872	86.2564	84.4140	78.9277

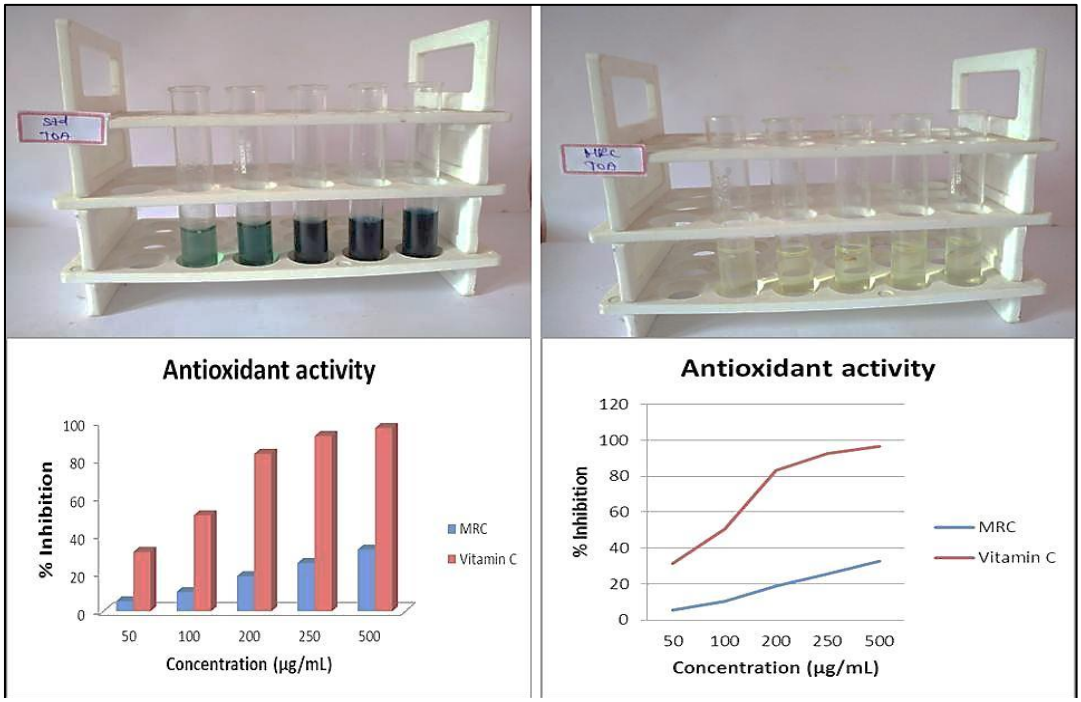

Figure:9 Antioxidant activity of Co_3O_4NPs by *Boerhavia diffusa* leaves extract

3.13 Antidiabetic activity

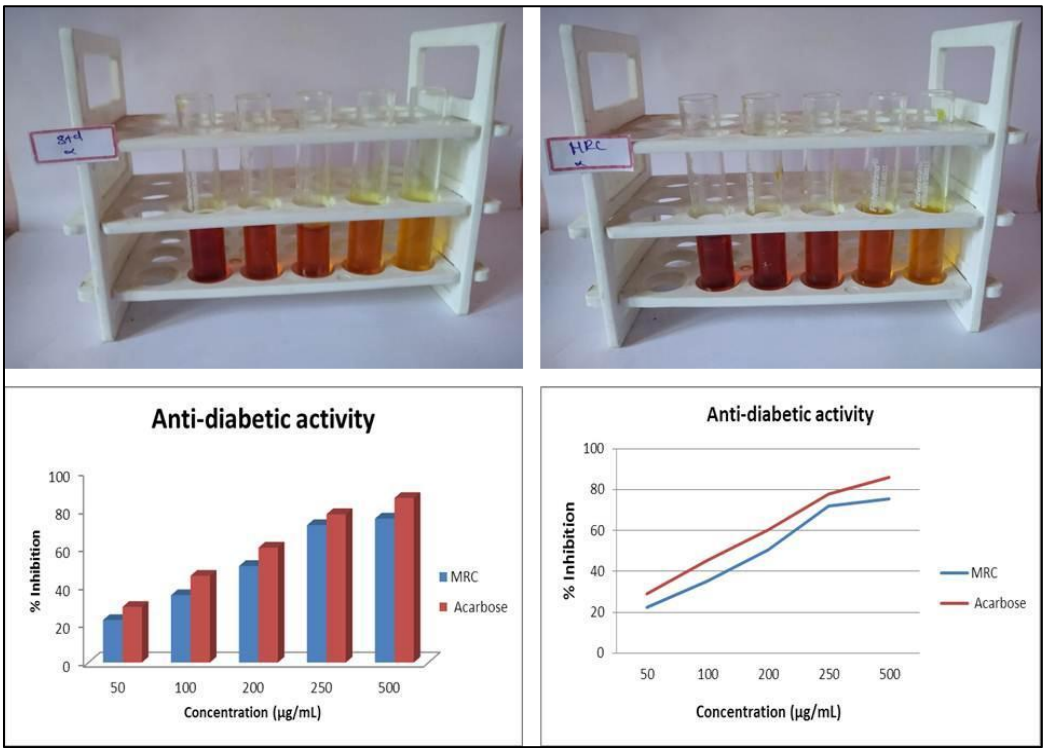

Figure:10 Anti diabetic activity of Co_3O_4NPs by *Boerhavia diffusa* leaves extract

The α -amylase inhibitory activity of Co_3O_4NPs with *Boerhavia diffusa* was studied,. The results exhibited a good significant inhibitory activity[56] against α-amylase enzyme of compounds Co_3O_4NPs when comparable with that of acarbose(Table:2., Figure.9.). Co_3O_4 NPs

showed notable significant inhibition activity, % inhibition 72 at 250 µg/mL, other concentrations are gradually increases with increased concentrations

3.14 Anti-inflammatory activity

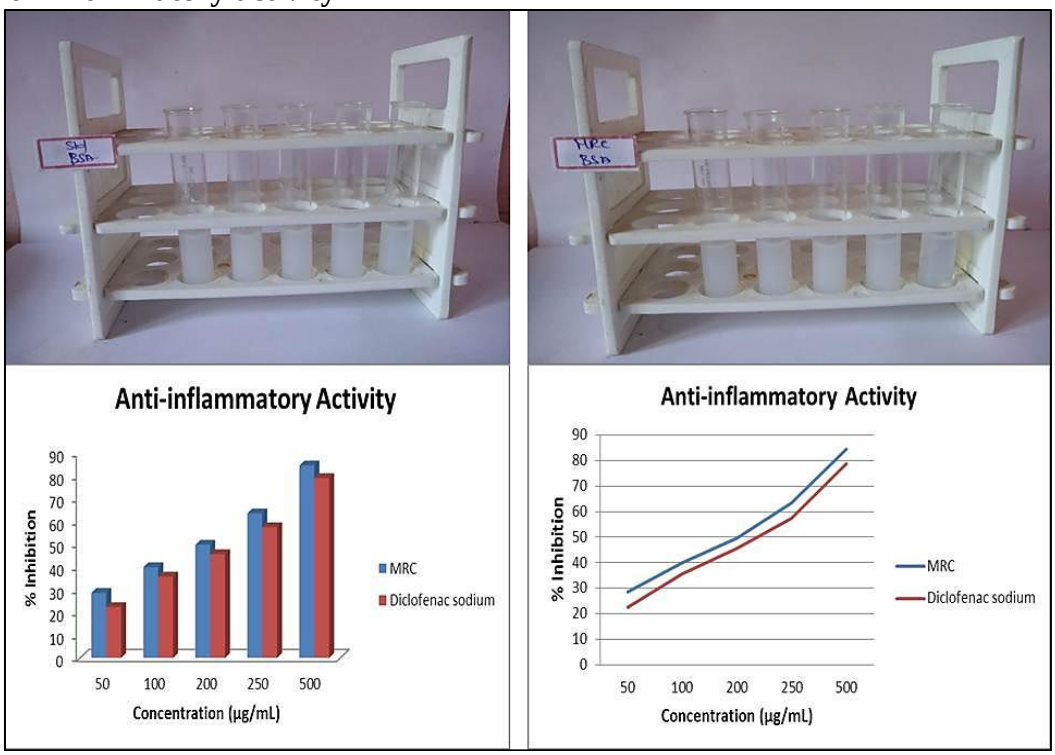

Figure:11 Anti-inflammatory activity of Co_3O_4NPs by *Boerhavia diffusa* leaves extract

The BSA denaturation technique used to measure the anti-inflammatory activity of green synthesized Co_3O_4NPs with *Boerhavia diffusa*. The results exhibited an excellent significant inhibitory activity[57] against BSA enzyme of compounds Co_3O_4NPs when comparable with that of diclofenac sodium(Table:2., Figure:11). The result reveals that extraordinary anti-inflammatory activity. Concentrations increases with increase of inhibition percentage.

3.15 Anticancer activity

Table:3 Percentage viability of Co_3O_4NPs of *Boerhavia diffusa* leaves extract

Concentration (µg/mL)	% Viability	
	Co_3O_4NPs	DOXORUBICIN
6.25	71.8299	57.6229
12.5	56.8050	45.9725
25	48.2494	35.9594
50	38.8296	27.0786
100	31.8628	17.9791

The *in vitro* anticancer study of Co_3O_4NPs was evaluated by MTT assay method. The nuclear staining results indicate the stimulation of apoptosis continued by necrosis in hepatocellular carcinoma cells by cobalt oxide nanoparticles. The anticancer effect of Co_3O_4NPs against HepG2 lines was performed the results show the good cytotoxic activity against the cancer cells. The concentration of Co_3O_4NPs play an important role in the anticancer activity. The Co_3O_4NPs are exhibits

the good results in the tested concentrations of 6.25 μg/ml, 12.5 μg/ml, 25 μg/ml, 50 μg/ml and 100 μg/ml.

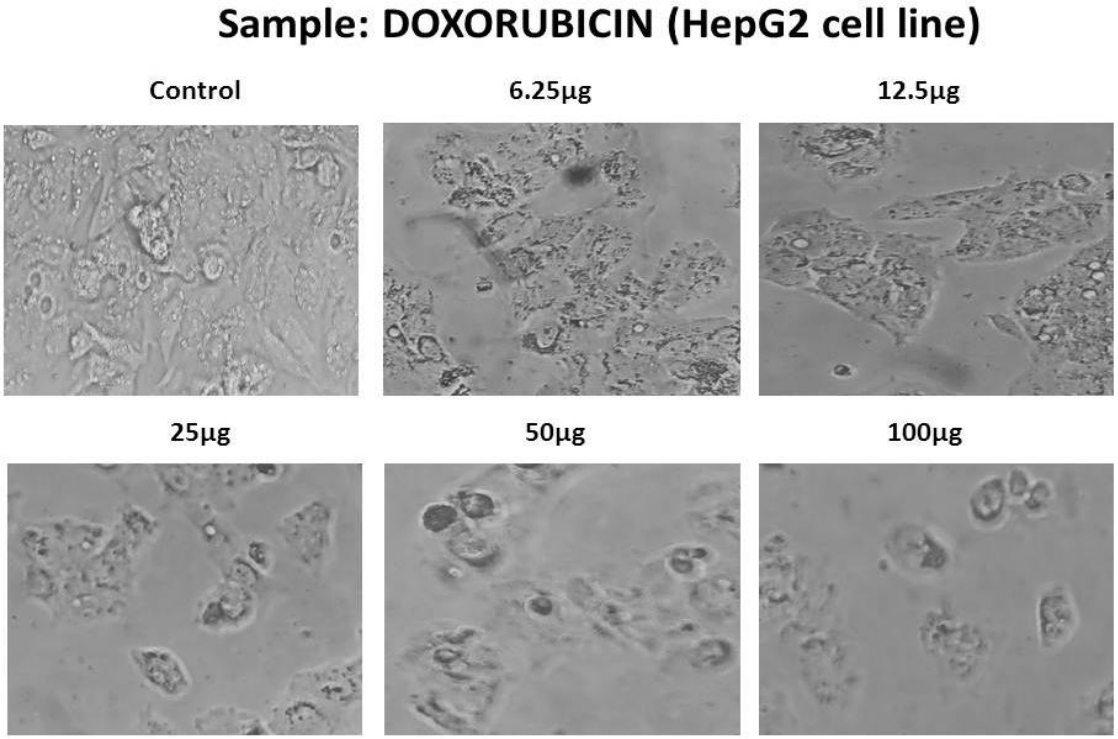

Figure:12 Anti-cancer activity of Standard drug Doxorubicin against HepG2 Cell line

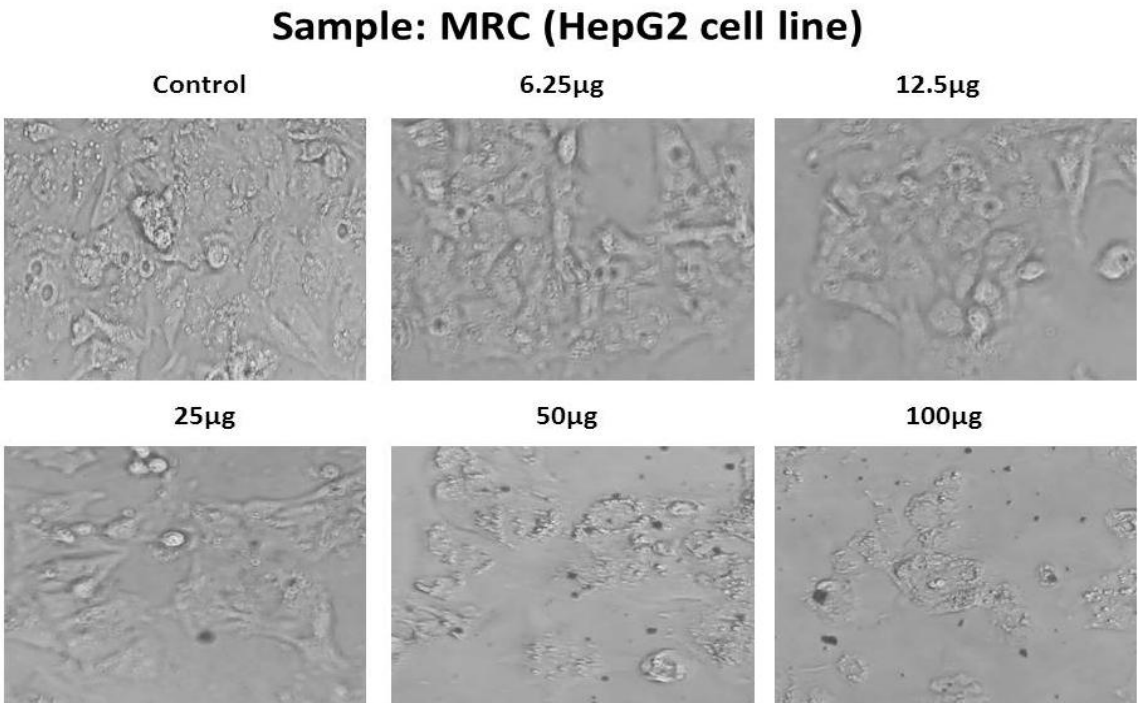

Figure:13 Anti-cancer activity of Co_3O_4NPs by *Boerhavia diffusa* leaves extract against HepG2 cell line

The lowest inhibitory action was observed form the concentration of 100 µg/ml. Our studies demonstrate the potential use of *Boerhavia diffusa* as a source of anti-cancer drug. The aqueous extract of the *Boerhavia diffusa* was tested for its cytotoxicity and apoptotic properties against the hepatocellular carcinoma (HepG2) cells in vitro. The anticancer activity was observed and that the synthesized cobaltoxide nanoparticles induce a dose dependent inhibition activity against HepG2 cells. Some of the approved chemotherapeutic agents were caused side effect and high cast. Therefore there is an important need to develop alternative medicines against this deadly disease [58]. Biosynthesis of Co_3O_4NPs using *Boerhavia diffusa* extract was developed in a very simple and eco-friendly method. Generally, plant extract containing proteins molecule containing phytoconstituents have played a major role in acting as a reductant as well as a capping material in order to synthesize Co_3O_4NPs that functioned effectively as an anticancer agent against HepG2 cancer cells. The control group of untreated HepG2 cells showed full spherical shaped and homogeneous pink nuclear staining. While the cells treated with cobalt oxide nanoparticles indicated an irregular shape nucleus, cell shrinkage and scattering of nuclear granules. It suggested the indication of nuclear fragmentation (figure 12). Hence, the treatment of Co_3O_4NPs *Boerhavia diffusa* induces cell death in HepG2 cells. The Co_3O_4NPs *Boerhavia diffusa* have shown excellent IC_{50} value (24.13) compared with standard Doxorubicin IC_{50} (9.93).The observations indicate that synthesized Co_3O_4NPs by *Boerhavia diffusa* (Mookirattai) have favorable in-vitro anticancer activity on Hepatocellular carcinoma cancer cells.

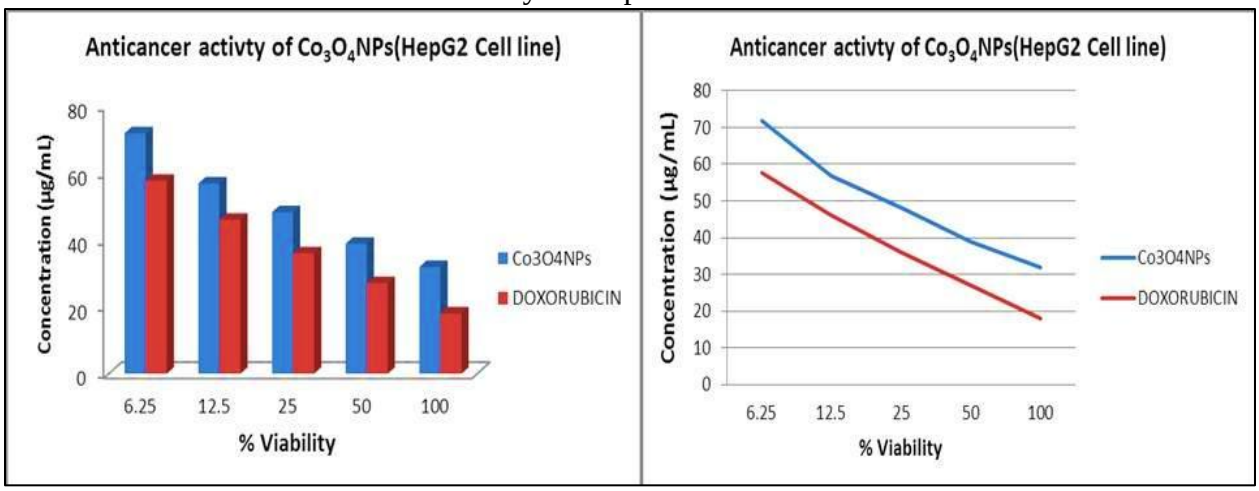

Figure:14 Cluster column chart of Anti-cancer activity of Co_3O_4NPs by *Boerhavia diffusa* leaves extract against HepG2 cell line

Conclusions

A green synthesis of Co_3O_4NPs was developed using aqueous leaves extract of *Boerhavia diffusa* was developed. The Co_3O_4NPs nanoparticles were obtained by cobalt nitrate hexahydrate in which the chemical component from aqueous leaves extract of *Boerhavia diffusa* act as reducing agents. UV spectral analysis have shown the absorption maximum at 395.05nm, FTIR spectral results have shown doublet sharp peak at 662 cm^{-1} and 566 cm^{-1} , the strong evidence for spinel structure present in Co_3O_4NPs. The fluorescence spectrum has shown the intensity in 804.5 nm. The average size of Co_3O_4NPs have shown almost the results obtained in XRD, DLS, SEM image have shown in polycrystalline structure, EDS results have given the composition of the cobalt and oxygen present in the nanoparticles. The TEM results reveals that trigonal, pentagonal and hexagonal shapes. Co_3O_4NPs having definite electrical properties. In *vitro* microbiological analysis of antibacterial activity has shown excellent results against *Staphylococcus aureus*. Highest antifungal activities have shown in Co_3O_4NPs *against Candida*

albicans. It is interestingly noted that the aqueous leaves extract of *Boerhavia diffusa reveals* very good antioxidant, antidiabetic and anti-inflammatory activities. The green synthesized Co_3O_4 NPs by *Boerhavia* inhibits the growth of HepG2 cancer cells and induces apoptosis in them due to their anticancer activity.

Reference

[1] Khan I, Saeed K, Khan I., *Arabian J Chem*. 12(7) (2019) 908–31.
[2] Nadeem M, Khan R, Afridi K, Nadhman A, Ullah S, Faisal S, *Int J Nanomed*. 15 (2020) 5951.
[3] Kubik T, Bogunia-Kubik K, Sugisaka M.,Curr Pharm Biotechnol.,6(1) (2005) 17–33.
[4] Smith DM, Simon JK, Baker Jr JR. *Nat Rev Immunol*.,13(8) (2013) 592–605.
[5] Faucon MP, Pourret O, Lange B. Cham: Springer, (2018) 233–9.
[6] Iravani S, Varma RS. Green Chem. 2020;22(9):2643–61.
[7] Egorova KS, Ananikov VP. Organometallics.;36(21) (2017) 4071–90.
[8] Xu Q, Li W, Ding L, Yang W, Xiao H, Ong WJ., Nanoscale.,11(4) (2019) 1475–504.
[9] Ansari SM, Bhor RD, Pai KR, Sen D, Mazumder S, Ghosh K, *Appl Surf Sci*.;414:(2017) 171–87.
[10] Raveau B, Seikh MM. *Z Anorg Allg Chem*.,641 (2015)1385–94.
[11] Bersuker IB., New York: Wiley; 1996.
[12] Liu J, Wang Z, Yan X, Jian P. *J Colloid Interface Sci*.505 (2017) 789–95.
[13] Su Y, Zhu Y, Jiang H, Shen J, Yang X, Zou W, Nanoscale.,6(24) (2014)15080–9.
[14] Azharuddin M, Zhu GH, Das D, Ozgur E, Uzun L, Turner AP, *Chem Commun*.;55(49): (2019) 6964–96.
[15] Cardoso VF, Francesko A, Ribeiro C, Bañobre-López M, Martins P, Lanceros-Mendez S. *Adv Healthcare Mater*. 7(5) (2018) 1700845.
[16] Liakos I, Grumezescu AM, Holban AM. *Molecules*. 19(8) (2014) 12710–26.
[17] Eleraky NE, Allam A, Hassan SB, Omar MM. *Pharmaceutics.* 12(2) (2020) 142.
[18] Jeevanandam J, Barhoum A, Chan Y S, Dufresne A, Danquah M K. *Beilstein Nanotechnol*. 9(1) (2018) 1050–74.
[19] Ahmad S, Munir S, Zeb N, Ullah A, Khan B, Ali J, *Int J Nanomed*.;14: (2019) 5087.
[20] Pachapur V, Brar SK, Verma M, Surampalli RY. *Am soci of civi eng libr*; 2015. 421–37.
[21] Khan I, Saeed K, Khan I. *Arabian J Chem.* 2017. doi: 10.1016/j.arabjc.2017.05.011.
[22] Ranjit K, Baquee AA. Nanoparticle: *Int Res J Pharm*.;12 (2013) 908–31.
[23] Anyaegbunam FN, Augustine C. *Dig J Nanomater Biostruct*.3(3) (2018) 847–56.
[24] Stella C, Soundararajan N, Ramachandran K.. AIP Adv;5(8) (2015) 087104.
[25] Korde P, Ghotekar S, Pagar T, Pansambal S, Oza R, Mane D. *J Chem Rev*.;2: (2020) 157–68.
[26] Li W, Jung H, Hoa ND, Kim D, Hong SK, Kim H. *Sens Actuators B*.;150(1) (2010)160–6.
[27] Li WY, Xu LN, Chen J. *Adv Funct Mater*. 15(5): (2005) 851–7.
[28] Kumar R, Kim HJ, Park S, Srivastava A, Oh IK. *Carbon*.;79: (2014)192–202.
[29] Adekunle AS, Oyekunle JA, Durosinmi LM, Oluwafemi OS, Olayanju DS, Akinola AS,. *Nano-Struct Nano-Objects*., 21 (2020) 100405.
[30] Hagelin-Weaver HA, Hoflund GB, Minahan DM, Salaita GN. *App Sur Sci*., 235(4) (2004) 420–48.

[31] Dekkers, S.; Wagner, J.G.; Vandebriel, R.J.; Eldridge, E.A.; Tang, S.V.Y.; Miller, M.R.; Römer, I.; de Jong, W.H.; Harkema, J.R.;Cassee, F.R. Part. *Fibre Toxicol*., 16 (2019) 39.
[32] Schuster, R.; Wähler, T.; Kettner, M.; Agel, F.; Bauer, T.;Wasserscheid, P.; Libuda, J. *Chem Open.*, 10 (2021) 141–152.
[33] Chekin, F., Vahdat, S.M. & Asadi, M.J. *Russ J Appl Chem*, 89 (2016) 816–822.https://doi.org/10.1134/S1070427216050219
[34] Kharade Suvarta D, Nikam Gurunath H., Mane Gavade Shubhangi J. Patil Sachinkumar R and Gaikwad Kishor V., *Res. J. Chem. Environ*., 24 (5) (2020) 9-13,
[35] Ali N.W., Al-Abdullah Z.T., Alabdulaziz B.A., Abood M. I.., Basrah Journal of Science., 39 (2) (2021) 292-305.
[36] He T, Chen D, Jiao X, Wang Y and Duan Y., *Chem. Mater.* 17 **(**15) (2005) 4023-30
[37] Khadhim A I, Kadhim R E., *Annals of R.S.C.B.*, 25(3) (2021) 5361 – 5372.,
[38] Dubey S, Kumar J, Kumar A, Sharma YC. *Adv Powd Tech*., 29(11) (2018) 2583–90.
[39] Salavati-Niasari M, Davar F, Mazaheri M, Shaterian M. Journal of Magnetism and Magnetic Materials., 320(3–4) (2008) 575–578.
[40] Herrero M, Benito P, Labajos F, Rives V. *Cata Today*., 128(3–4): (2007) 129–137.
[41] Treguer M., Rocco F., Lelong G., L. Nestour A., Cardinal T., Maali A and Lounis B., *Solid State Sci*., 7 (2005) 812-818.
[42] Zhu J., Tu W., Pan H., Zhang H., Liu B., Cheng Y, Zhao D, Zhang H., ACS Nano 14 (2020) 5780–5787.
[43] Aliyaa A. Urabe and Wisam J. Aziz., WNOFNS., 24 (2019) 356-364.
[44] Malathy D., Revathi M. *Research J. Pharm. and Tech*., 14(3) (2021) 1530-1534.
[45] Pusey, P.N. *Current Opinion in Colloid & Interface Science*., 4 (3) (1999) 177–185.
[46] Sirajul Haq, Farwah Abbasi, Manel Ben Ali, Amor Hedfi2, Amine Mezni, Wajid Rehman, Muhammad Waseem, Abdul Rehman Khan and Hamayun Shaheen., *Mater. Res. Express* 8 (2021) 075009.
[47] Wang X, Zhong Y, Zhai T, Guo Y, Chen S, Ma Y, Yao J, Bando Y, Golberg, D., *J. Mater. Chem*., 21 (2011**)** 17680–17687.
[48] Xiao X, Liu X, Zhao H, Chen D, Liu F, Xiang J, Hu Z, Li Y., *Adv. Mater*., 24, (2012) 5762–5766.
[49] Shen, X.-P.; Miao, H.-J.; Zhao, H.; Xu, Z. *Appl. Phys. A*, 91 (2008) 47–51.
[50] Wang, R.; Liu, C.; Zhang, H.; Chen, C.; Guo, L.; Xu, H.; Yang, S. *Appl. Phys. Lett*. 85, (2004) 2080–2082.
[51] Chen, Y.H.; Zhou, J.F.; Mullarkey, D.; O'Connell, R.; Schmitt,W.; Venkatesan, M.; Coey, M.; Zhang, H.Z. *AIP Adv*., 5 (2015) 087122.
[52] Mogomotsi R N, Akinola S S, Emeka E E, and Fayemi O E., *Mater. Res. Express*, 7 (2020) 055001
[53] Maouche N, Nessark B., *Int J Electrochem*, , Article ID 670513, (2011) 5.
[54] Supraja N., Prasad T.N.V.K.V., Soundariya M. and Babujanarthanam R., *AIMS Bioeng*, 3 (4) (2016) 425-440.
[55] Ajarem J.S, Maodaa S.N, Allam A.A, Taher M.M, Khalaf M. Benign., *J Clust Sci*., 33(2) (2022) 717‑28.
[56] Preety R, Roy Anitha, Rajeshkumar S, Lakshmi T., *Int. J. Res. Pharm. Sci.*, 11(2) (2020) 1267-1269.
[57] Govindappa M, Hemashekhar B, Arthikala M, Ravishankar Rai V., Ramachandra Y.L., *Results in Physics* 9 (2018) 400–408.
[58] Yang H, Hu Y, Zhang X, Qiu G., *Mater Lett*, 58 (2004) 387–389.